

Identification of coupling direction: Application to cardiorespiratory interaction

Michael G. Rosenblum*

Department of Physics, University of Potsdam, Am Neuen Palais, PF 601553, D-14415 Potsdam, Germany

Laura Cimponeriu and Anastasios Bezerianos

Department of Medical Physics, University of Patras, 26 500 Rion Patras, Greece

Andreas Patzak and Ralf Mrowka

Charité, Johannes-Müller Institute for Physiology, Humboldt University, Tucholsky Strasse 2, D-10117 Berlin, Germany

(Received 4 December 2001; published 28 March 2002)

We consider the problem of experimental detection of directionality of weak coupling between two self-sustained oscillators from bivariate data. We further develop the method introduced by Rosenblum and Pikovsky [Phys. Rev. E **64**, 045202 (2001)], suggesting an alternative approach. Next, we consider another framework for identification of directionality, based on the idea of mutual predictability. Our algorithms provide directionality index that shows whether the coupling between the oscillators is unidirectional or bidirectional, and quantifies the asymmetry of bidirectional coupling. We demonstrate the efficiency of three different algorithms in determination of directionality index from short and noisy data. These techniques are then applied to analysis of cardiorespiratory interaction in healthy infants. The results reveal that the direction of coupling between cardiovascular and respiratory systems varies with the age within the first 6 months of life. We find a tendency to change from nearly symmetric bidirectional interaction to nearly unidirectional one (from respiration to the cardiovascular system).

DOI: 10.1103/PhysRevE.65.041909

PACS number(s): 87.90.+y, 05.45.Tp, 05.45.Xt, 05.40.Ca

I. INTRODUCTION

Theoretical insights in nonlinear dynamics have been widely used in time series analysis [1]. In particular, the concepts of generalized [2] and phase [3–5] synchronization have been exploited for the identification of interdependences between coupled sub(systems) from multivariate data and have found a number of applications in the studies of biological time series [5–11]. One can formulate two main problems in such an analysis. The first problem is to reveal whether the systems under investigation are coupled and to quantify the intensity of interaction, while the second one is to characterize the driver-response (causal) relationships, or directionality of coupling.

Many natural phenomena can be modeled by coupled irregular self-sustained oscillators. The description of a weak interaction between such systems can be reduced to the phase dynamics [5,12]. Hence, if one considers an inverse problem—characterization of weak coupling from data—it is sufficient to analyze interrelation between the phases ϕ of oscillators; the phases can be beforehand estimated from the scalar signals. In this way, the intensity of interaction can be assessed quantitatively [5,9,11]. Moreover, a recent approach [13] demonstrated that the asymmetry in interaction of two oscillators could be also detected. The idea of this approach is as follows: if, say, system 1 is driven by system 2, then the evolution of ϕ_1 depends also on ϕ_2 ; in other words, prediction of ϕ_1 from its previous values can be improved by taking into account the prehistory of ϕ_2 only if system 2 drives system 1.

In the present paper we further develop the technique for detection of the directionality in coupling. We propose two algorithms and compare them with that of Ref. [13]. Next, we exploit the presented method to address an important physiological problem—analysis of the direction of the cardiorespiratory interaction.

Different aspects of interaction between cardiovascular and respiratory systems in humans have been the subject of interest of many researchers. In physiological terms, there are different levels where interaction between heart rate and respiratory rhythm might occur. Foremost, the central nervous interaction in the cardiorespiratory region in the brain stem plays an eminent role. A well-studied phenomenon is the modulation of the heart rate by respiration, known since 19th century as respiratory sinus arrhythmia [14]. Another possible effect of interaction is synchronization. So, 1:m locking between the cardiac and respiratory rhythms was investigated in Ref. [15]. Graphical tools and quantification measures allowing one to assess the general case of interaction with $n:m$ frequency relation were introduced in [8,10,11] and used in Ref. [16]. In our previous work [17], we analyzed cardiorespiratory interaction in a large group of healthy infants and we found that intensity of interaction increased with the age.

It is widely believed that coupling between the cardiovascular and respiratory system is unidirectional, i.e., the respiratory rhythm influences the heart rate via vagal stimulation and direct mechanical action on the primary cardiac pacemaker, the sinus node; this is called irradiation theory. Nevertheless, some evidence [18] conflicts with this theory suggesting that the respiratory oscillator in the central nervous system is not always dominant, i.e., the cardiorespiratory

*Electronic address: www.agnld.uni-potsdam.de

coupling is bidirectional. To obtain further insight into this controversy, we investigated the direction in cardiorespiratory interaction in healthy babies and its age dependence. We show that within the first 6 months of life there is a tendency to change from roughly symmetric interaction to a nearly unidirectional one (from respiration to heart rate). Furthermore, our directionality indices clearly demonstrate a dependence on breathing frequency. We explain this dependence by two classes of frequency response properties of the pathway transmitting information from the central nervous system to the heart.

The paper is organized as follows. In Sec. II, we present our techniques of data analysis and discuss their relation to other methods; in Sec. III, we illustrate the techniques by several model examples; in Sec. IV, we describe and discuss the analysis of experimental data; and in Sec. V, we summarize our results.

II. TECHNIQUES OF DATA ANALYSIS

Estimation of interdependence between two time series is a traditional problem of signal processing. Widely used tools such as cross spectra [19], mutual information [20] or maximal correlation [21] provide *symmetric* measures and are, therefore, not suitable for evaluation of *causality* in interrelation. The latter issue was addressed in recent studies, where one can outline two main approaches. One approach, based on the information theory, used entropy measures [22]. A second approach, arising from studies of generalized synchronization, exploited the idea of mutual predictability: it quantified the ability to predict the state of the first system from the knowledge of the second one [6]. While both approaches are rather complicated to implement and interpret, neither requires any assumptions on the systems under investigation. On the contrary, the approach to analysis of causality or directionality of interaction, introduced in Ref. [13] and further developed here, is explicitly based on the assumption that experimentalists deal with weakly interacting self-sustained oscillators. In this particular, but pretty often encountered case the direction of coupling can be efficiently quantified.

The main idea of Ref. [13] is to use the fact that weak coupling affects the phases of interacting oscillators, whereas the amplitudes remain practically unchanged [5,12]. Hence, the dynamics can be reduced to those of two phases $\phi_{1,2}$:

$$\dot{\phi}_{1,2} = \omega_{1,2} + \varepsilon_{1,2} f_{1,2}(\phi_{2,1}, \phi_{1,2}) + \xi_{1,2}(t). \quad (1)$$

Here, random terms $\xi_{1,2}$ describe noisy perturbations that are always present in real-world systems; small parameters $\varepsilon_{1,2} \ll \omega_{1,2}$ characterize the strength of the coupling. Equation (1) describes also the phase dynamics of coupled continuous-time chaotic systems; in this case $\xi_{1,2}$ are irregular terms that reflect the chaotic nature of amplitudes [3]. The fact that the regular component of the phase dynamics is two dimensional, essentially simplifies detection of the asymmetry in interaction. Functions $f_{1,2}$ are 2π periodic in both arguments and combine the description of the phase dynamics of autonomous (uncoupled) systems and the coupling between

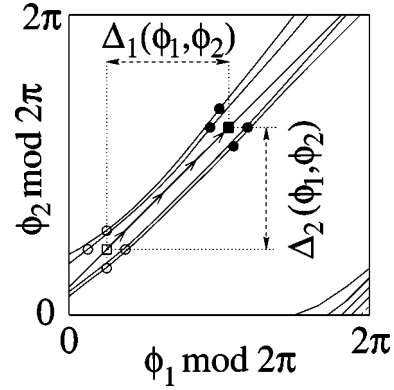


FIG. 1. Evolution of trajectories of system (1) on the torus (ϕ_1, ϕ_2) (schematically). Open symbols show some arbitrarily taken points, closed symbols show the positions of these points after time interval τ , where τ is a parameter; evolution of one point (boxes) is shown by arrows. Phase increment $\Delta_1 = \phi_1(t + \tau) - \phi_1(t)$ depends on both ϕ_1, ϕ_2 if there is a driving from system 2 to system 1, and only on ϕ_1 if 2 does not act on 1 (similarly for Δ_2). Thus, analysis of dependences $\Delta_{1,2} = F_{1,2}(\phi_{1,2}, \phi_{2,1})$ helps to reveal and quantify asymmetry in the coupling between two oscillators; smooth functions $F_{1,2}$ are obtained by an approximation. Note that $\Delta_{1,2}$ are computed with account of possible trajectory revolution around the torus, so that generally $\Delta_{1,2} > 2\pi$.

them. If the coupling is bidirectional, f_1 and f_2 depend on both ϕ_1 and ϕ_2 . In case of unidirectional driving, say from system number 1 to system number 2, $f_1 = f_1(\phi_1)$, whereas $f_2 = f_2(\phi_1, \phi_2)$ is the function of two arguments.

In the following discussion of the algorithms, we assume that the time series of phases are known. Practically, the phases $\phi_{1,2}(t_k)$, $t_k = k\Delta t$, $k = 1, 2, \dots$, where Δt is the sampling interval, can be estimated from the experimental data as discussed in Sec. IV.

A. Evolution map approach (EMA)

Here we briefly describe the technique introduced in Ref. [13], we call it the EMA. Let us consider increments of phases during some fixed time interval τ (Fig. 1):

$$\Delta_{1,2}(k) = \phi_{1,2}(t_k + \tau) - \phi_{1,2}(t_k), \quad (2)$$

the choice of the parameter τ is discussed below. Note that the phases are unwrapped, i.e., not reduced to the interval $[0, 2\pi)$; hence $\Delta_{1,2}$ can be larger than 2π . These increments can be considered as generated by some unknown two-dimensional noisy map

$$\Delta_{1,2}(k) = \omega_{1,2}\tau + \mathcal{F}_{1,2}(\phi_{2,1}(t_k), \phi_{1,2}(t_k)) + \eta_{1,2}(t_k). \quad (3)$$

The deterministic parts $\mathcal{F}_{1,2}$ of the map can be estimated from the time series $\Delta_{1,2}(k)$ and $\phi_{1,2}(k)$. For this purpose, we fit (in the least mean square sense) the dependences of Δ_1 and Δ_2 on ϕ_1, ϕ_2 . As the phases are cyclic variables, the natural choice of the probe function is a finite Fourier series, $F_{1,2} = \sum_{m,l} A_{m,l} e^{im\phi_1 + il\phi_2}$. Note that fitting also filters out the

noise. A similar procedure was used for noise reduction in discrete dynamical systems [23] and (with $\tau \rightarrow 0$) for extracting model equations from experimental noisy data [24].

From the smooth functions $F_{1,2}$ obtained via approximation one can compute the measures $c_{1,2}$ of the cross dependences of phase dynamics of two systems

$$c_{1,2}^2 = \int \int_0^{2\pi} \left(\frac{\partial F_{1,2}}{\partial \phi_{2,1}} \right)^2 d\phi_1 d\phi_2. \quad (4)$$

Finally, the *directionality index* is introduced as

$$d^{(1,2)} = \frac{c_2 - c_1}{c_1 + c_2}. \quad (5)$$

Normalized in this way, the index varies from 1 in the case of unidirectional coupling ($1 \rightarrow 2$) to -1 in the opposite case ($2 \rightarrow 1$) with intermediate values $-1 < d^{(1,2)} < 1$ corresponding to bidirectional coupling. Note that the index is an integrated measure of how strong each system is driven and of how sensitive it is to the drive.

To understand exactly how the asymmetry in coupling is characterized by the index d , i.e., how d is related to the parameters of the model equation (1), we estimate the deterministic components $\Delta_{1,2}$ of the phase increase within the interval τ . As follows from Eq. (1), in the absence of noise, we obtain for small $\varepsilon_{1,2}$,

$$\begin{aligned} \Delta \phi_{1,2} &\approx \omega_{1,2} \tau + \varepsilon_{1,2} \int_0^\tau f_{1,2}(\phi_{2,1}, \phi_{1,2}) dt \\ &= \omega_{1,2} \tau + \mathcal{F}_{1,2}(\phi_{2,1}, \phi_{1,2}). \end{aligned} \quad (6)$$

So, for a particular (but rather common) case of antisymmetric coupling function $f_1(\phi_2, \phi_1) = -f_2(\phi_1, \phi_2)$, we obtain from Eq. (4) $c_{1,2} = a \varepsilon_{1,2}$, where the constant a is determined by the integral in Eq. (6). In general case the coefficients $c_{1,2} = a_{1,2} \varepsilon_{1,2}$, where $a_1 \neq a_2$ reflect also the difference in coupling functions $f_{1,2}$. Thus, the directionality index d characterizes the asymmetry in coupling but does not incorporate the difference in the frequencies of autonomous systems.

B. Instantaneous period approach (IPA)

Let us now compute the time needed for the phase $\phi_{1,2}(t_k)$ to increase by 2π ; in other words, we compute the instantaneous periods or Poincaré return times, for all k [25]. Obviously, for uncoupled noisy and/or chaotic systems the return times fluctuate around a constant (mean period), $T_{1,2}(k) = T_{1,2}^0 + \eta_{1,2}(t_k)$, while for coupled systems $T_{1,2}(k) = T_{1,2}^0 + \Theta_{1,2}[\phi_{2,1}(t_k), \phi_{1,2}(t_k)] + \eta_{1,2}(t_k)$. The deterministic component $\Theta_{1,2}$ of this dependence can be again found by fitting a Fourier series, and the cross dependences of T_1 on ϕ_2 and of T_2 on ϕ_1 can be characterized in the same way as above, by computing coefficients $c_{1,2}$ from partial derivatives of $\Theta_{1,2}$ with respect to $\phi_{2,1}$, similar to Eq. (4). Then, the new directionality index $r^{(1,2)} = (c_2 - c_1)/(c_2 + c_1)$ is computed

[cf. Eq. (5)]. An important advantage of the proposed algorithm is the absence of parameters.

Now we show that this algorithm provides different characterization of asymmetry than EMA. Indeed, for weak coupling, $\varepsilon_{1,2} \ll \omega_{1,2}$, the deterministic component of the instantaneous period T_1 can be estimated from Eq. (1) as

$$\begin{aligned} T_1(\phi_1, \phi_2) &= \int_{\phi_1}^{\phi_1+2\pi} \frac{d\phi'}{\omega_1 + \varepsilon_1 f_1(\phi_2, \phi')} \\ &= \frac{1}{\omega_1} \int_{\phi_1}^{\phi_1+2\pi} \frac{d\phi'}{1 + \frac{\varepsilon_1}{\omega_1} f(\phi_2, \phi')} \\ &= \frac{2\pi}{\omega_1} - \frac{\varepsilon_1}{\omega_1^2} \int_{\phi_1}^{\phi_1+2\pi} f(\phi_2, \phi') d\phi' \\ &= T_1^0 + \Theta_1(\phi_2, \phi_1), \end{aligned} \quad (7)$$

and similarly for T_2 . Clearly, for coupling functions satisfying $f_1(\phi_2, \phi_1) = -f_2(\phi_1, \phi_2)$, this algorithm provides $c_{1,2} = a \varepsilon_{1,2} / \omega_{1,2}^2$. Hence, directionality index r reflects not only asymmetry in coupling coefficients $\varepsilon_{1,2}$ and asymmetry in coupling functions $f_{1,2}$, but also in natural frequencies $\omega_{1,2}$.

C. Mutual prediction approach (MPA)

As already mentioned, mutual prediction is used for estimation of causal relations in the methods based on the concept of generalized synchronization. These methods imply existence of a functional relationship between the (phase) states of two systems; such a relation arises due to a comparatively strong coupling. We exploit here a different understanding of mutual prediction, and this allows us to assess a weaker interaction. Namely, we look whether the predictability of, say, first time series can be improved by the knowledge of the second signal. A similar concept, initially introduced in Ref. [26] was very recently used by several groups [27,28]. The main distinction of our approach is that we work with phases, not with raw signals.

Thus, we take one series, say, $\phi_1(t_k)$ and use some scheme to predict a future of its points. For the k th point we compute the *univariate prediction error* $E_1(t_k) = |\phi_1'(t_k) - \phi_1(t_k + \tau)|$, where $\phi_1'(t_k)$ is the τ -step ahead prediction of the point $\phi_1(t_k)$; remember that phases are unwrapped. Next, we repeat the prediction for $\phi_1(t_k)$, but this time we use both signals ϕ_1, ϕ_2 for construction of the predictor. In this way we obtain the *bivariate prediction error* $E_{12}(t_k)$. If system 2 influences the dynamics of system 1 then we expect $E_{12}(t_k) < E_1(t_k)$, otherwise (for sufficient statistics) $E_{12}(t_k) = E_1(t_k)$. The root mean squared $E_1(t_k) - E_{12}(t_k)$, computed over all possible k and denoted by I_{12} , quantifies the *predictability improvement* for the first signal. This measure characterizes the degree of influence of the second system on the first one. Computing in the same way I_{21} , we end with the directionality index

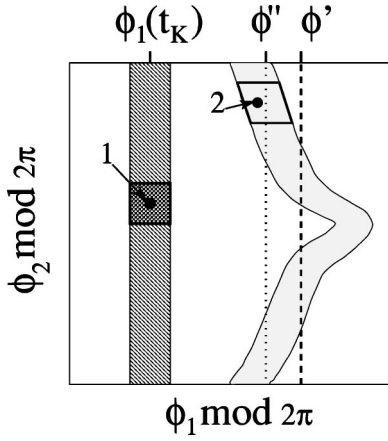


FIG. 2. Illustration of the mutual prediction approach. A chosen point, $\phi_1(t_K)$, evolves during the time interval τ from position 1 to position 2; the points that have close ϕ_1 coordinate (delineated vertical stripe) evolve to the dotted stripe. The average of these evolved states gives a univariate prediction ϕ' . A better prediction ϕ'' can be obtained using only the points that have close coordinates in both ϕ_1 and ϕ_2 , i.e., points in a square neighborhood of point 1. Note that the stronger is the dotted stripe bent, the larger is the predictability improvement. As follows from Eq. (6), this bending is proportional to ε_1 ; hence, the index $p^{(1,2)}$ quantifies bidirectional coupling in the same way as the index $d^{(1,2)}$.

$$p^{(1,2)} = \frac{I_{21} - I_{12}}{I_{12} + I_{21}}. \quad (8)$$

Particularly, we use simple prediction scheme due to the low dimension of the phase dynamics. In constructing predictor, we exploit a common idea that similar states have similar future. So, we pick up one point of the signal $\phi_1(t_k)$, say at the time t_K and search for all points in the signal that have value close to the chosen point; important that here the phases are taken in $[0, 2\pi)$ and the distances between points are defined on the unit circle. Namely, for a chosen point $\phi_1(t_K)$ we find all points $\phi_1(t_l)$ such that $|e^{i\phi_1(t_l)} - e^{i\phi_1(t_K)}| < \delta$, where δ is a constant; these points form a stripe on the (ϕ_1, ϕ_2) torus (see Fig. 2). Then we compute the predicted phase increment $\Delta'_1(K) = \langle \Delta_1(l) \rangle$, where $\Delta_1(l)$ are phase increments [see Eq. (2)], and $\langle \rangle$ denotes averaging. Univariate prediction error $E_1(K)$ is then $|\Delta'_1(K) - \Delta_1(K)|$. To make the bivariate prediction, we choose among t_l the subset of points t_m (mutual neighbors) satisfying $|e^{i\phi_2(t_m)} - e^{i\phi_2(t_K)}| < \delta$, and proceeding as described above, compute the error E_{12} [29]. The errors E_2, E_{21} corresponding to the signal $\phi_2(t_k)$ are obtained in a similar way.

Several remarks are in order. First, the described scheme can be understood as a kind of local (constant) approximation technique. Generally, different prediction schemes can be used to estimate directionality. Second, as we are interested in the predictability improvement, not in the predictability itself, it is not required to search for the optimal prediction scheme. Finally, we emphasize that the MPA does not directly use the assumption of weakly coupled oscillators; generally, it can be applied to arbitrary signals. If the as-

sumption of weak coupling is correct, then the choice of phases is crucial as these variables are mostly sensitive to the coupling.

To summarize this section, we emphasize two points. First, it is clear that all methods fail if oscillators synchronize. Indeed, in this case $\phi_{1,2}$ are functionally related, and no information on the coupling direction can be obtained [30]. Practically it means that the points on the (ϕ_1, ϕ_2) torus collapse to a line, and the approximation procedure fails. Thus, the direction of interaction can be revealed if the coupling is too weak in order to induce mode locking (i.e., in the quasiperiodic state) or the noise in the system is strong enough to cause large deviations from the synchronous state. If the noisy systems are close to a synchronous state, the points on the torus form a band with some (rare) excursions from it. In this case the described global approximation procedures, i.e., EMA and IPA are not efficient and a scheme based on local approximation is required. Next, we emphasize that there is no unique way to quantify the directionality in case of bidirectional coupling; different methods can, therefore, give noncoinciding characteristics (e.g., d and r indices do not coincide). The choice of a quantification measure is to large extent a matter of taste.

III. TESTS OF ALGORITHMS WITH SIMULATED DATA

In this section we illustrate the introduced algorithms by application to simulated data and discuss the choice of parameters. Note that the IPA is parameter free, EMA has only one parameter τ , and MPA has two parameters τ and radius of the neighborhood δ . Next, we briefly discuss the case when the frequencies of two oscillators are essentially different and the case of more than two interacting systems. We especially pay attention to the case of short and noise contaminated data. The ability of the techniques to work with such records is particularly important for biomedical applications.

A. Two coupled phase oscillators

We start, following Ref. [13] with the model of coupled noisy phase oscillators:

$$\dot{\phi}_{1,2} = \omega_{1,2} + b \cos(\phi_{1,2}) + \varepsilon_{1,2} \sin(\phi_{2,1} - \phi_{1,2}) + \xi_{1,2}(t), \quad (9)$$

where $\phi_{1,2}$ are phase variables evolving on a two-dimensional torus, parameters $\omega_{1,2}$ govern the natural frequencies of oscillators (although do not coincide with them for $b \neq 0$), $\varepsilon_{1,2}$ are the coupling coefficients, and $\xi_{1,2}$ are noise terms. In the following simulations $\xi_{1,2}$ are Gaussian δ -correlated noise terms, $\langle \xi_i(t) \xi_j(t') \rangle = 2D \delta(t-t') \delta_{i,j}$. The model (9) describes the phase dynamics in the general case of weakly coupled noisy limit cycle oscillators [12]; it also appears in the description of interacting continuous-time chaotic systems, Josephson junction arrays [31], and phase-locked loops [32].

First, we consider the effect of noise on the estimates of directionality (Fig. 3). The parameters of the system (9) are

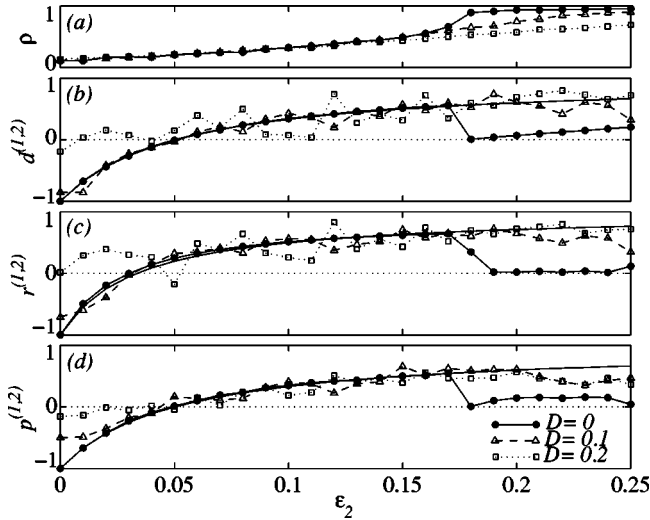


FIG. 3. Effect of noise on the estimation of directionality indices. One coupling coefficient is kept constant, $\varepsilon_1=0.05$, whereas the second coefficient is gradually varied. The indices are shown in (b)–(d) for different values of noise intensity. The solid curves show the dependence $y=(\varepsilon_2-\varepsilon_1)/(\varepsilon_2+\varepsilon_1)$ in (b),(d) and $y=(\varepsilon_2\omega_1^2-\varepsilon_1\omega_2^2)/(\varepsilon_2\omega_1^2+\varepsilon_1\omega_2^2)$ in (c). The degree of synchronization can be traced by the synchronization index ρ (a). In the absence of noise, all indices correctly reflect the asymmetry in interaction as long as the system remains in the quasiperiodic state (for $\varepsilon_2 < \approx 0.17$); noise helps to estimate the indices for $\varepsilon_2 > 0.17$, causing deviations from the synchronous regime.

$\omega_{1,2}=1 \pm 0.1$, $b=0.5$. Coupling coefficient ε_1 is fixed at 0.05 while ε_2 is varied in the interval $[0, 0.25]$ and three directionality indices $d^{(1,2)}$, $r^{(1,2)}$, and $p^{(1,2)}$ are computed for different values of the noise intensity D . For the noise-free case, all indices correctly recover the information on the asymmetry of coupling as long as the system remains in a quasiperiodic state (for $\varepsilon_2 < \approx 0.17$). The estimated indices $d^{(1,2)}$ and $p^{(1,2)}$ closely follow the theoretical curve

$$\frac{\varepsilon_2 - \varepsilon_1}{\varepsilon_1 + \varepsilon_2}, \quad (10)$$

whereas the index $r^{(1,2)}$ follows

$$\frac{\varepsilon_2\omega_1^2 - \varepsilon_1\omega_2^2}{\varepsilon_1\omega_2^2 + \varepsilon_2\omega_1^2}. \quad (11)$$

The performance of all algorithms degrade rapidly with the synchronization transition (traced by means of the synchronization index ρ [33]). Indeed, direction of interaction cannot be estimated in case of synchronization, when phases $\phi_{1,2}$ are functionally related. The influence of noise is twofold. On one hand, it naturally makes the estimation less precise, especially for very weak coupling [clearly, correct estimation is not possible if the noise term in Eq. (9) is in average larger than the coupling]. On the other hand, noise facilitates estimation of the indices for larger coupling values (correspon-

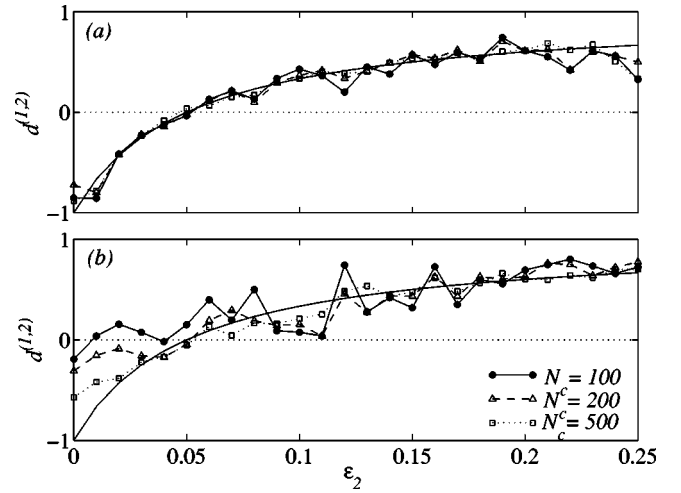


FIG. 4. Effect of data length on the estimation of directionality index d for noise intensity $D=0.1$ (a) and $D=0.2$ (b). The estimates are shown for different numbers of cycles N_c in the data; the solid line shows the dependence $y=(\varepsilon_2-\varepsilon_1)/(\varepsilon_2+\varepsilon_1)$.

dent for the synchronized regimes in the noise-free system). Note that the records used for estimation of indices contain only ≈ 100 periods of oscillations; with such short records, the MPA approach works better in the noisy case. Increase of the data length allows for better estimation of directionality from noisy data, the corresponding results are shown in Fig. 4.

Now we discuss the selection of parameters for EMA and MPA, starting with the parameter τ . Clearly, the value of τ should be related to the periods of oscillation $\tau=T_{1,2}$. Indeed, the influence on the own dynamics of an oscillator [note the $b \cos(\phi_{1,2})$ term in Eq. (9)] averages out during each cycle. As the frequencies of two oscillators are differ-

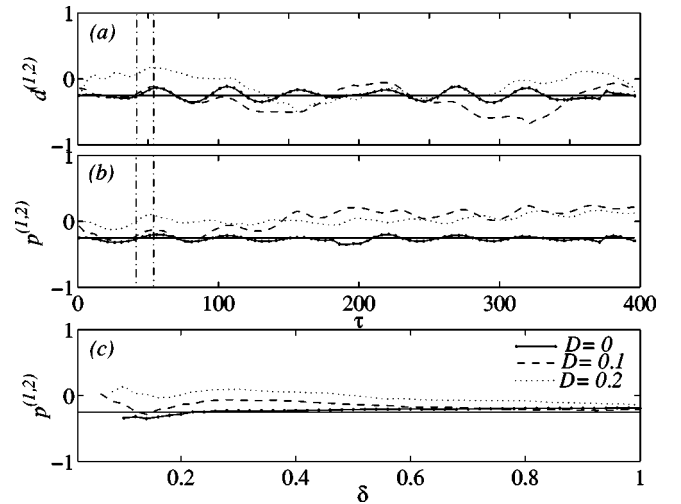


FIG. 5. Dependence of d and p indices on parameters for one coupling configuration ($\varepsilon_1=0.05, \varepsilon_2=0.03$) and different levels of noise. (a) d vs τ , (b) p vs τ for $\delta=0.3$, and (c) p vs δ for $\tau=(T_1+T_2)/2$. The vertical dashed lines in (a),(b) show the values corresponding to mean oscillation periods of both systems.

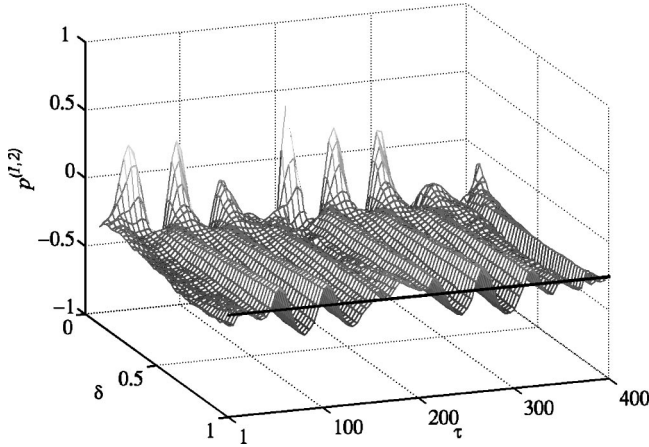


FIG. 6. Dependence of p index on parameters δ and τ for one coupling configuration ($\varepsilon_1=0.05, \varepsilon_2=0.03$) in the absence of noise.

ent, we have to find a compromise. Our tests suggest the following choice: $\tau = \min(T_1, T_2)$ and $\tau = (T_1 + T_2)/2$ for EMA and MPA, respectively. The computed dependences of d and p indices on τ are shown in Figs. 5(a), 5(b) for different levels of noise. Regarding the parameter δ , we emphasize two counteracting tendencies: δ should be small enough to resolve the influence of coupling and large enough in order to cope with the noise contamination dominating at small scales; the computed dependences are shown in Fig. 5(c) and Fig. 6. Clearly, short records require larger δ . Note that by definition $0 < \delta < 2$.

We have also tested the algorithms in case when the natural frequencies of coupled oscillators are essentially different, $\omega_1 \approx 0.4$, $\omega_2 \approx 1.2$, $b=0$. The computations show that the indices follow the theoretical curves (10) and (11) in this case as well. Note, that these curves are now essentially different due to the factor ω_1/ω_2 . In conclusion, tests with the data generated by two coupled phase oscillators demonstrate that all indices allow reliable estimate of the asymmetry in coupling from short noisy data.

B. Asymmetric coupling

We discuss now the case of asymmetric coupling. For the sake of definiteness, we consider $f_1 = \sin(\phi_2 - 3\phi_1)$, $f_2 = \sin(3\phi_1 - \phi_2)$. Clearly, in computation of the coefficient c_2 according to Eq. (4) we obtain, due to derivation, an additional factor of 3. Hence, the indices $d^{(1,2)}$ and $r^{(1,2)}$ follow now the dependences $(3\varepsilon_2 - \varepsilon_1)/(\varepsilon_1 + 3\varepsilon_2)$ and $(3\varepsilon_2\omega_1^2 - \varepsilon_1\omega_2^2)/(\varepsilon_1\omega_2^2 + 3\varepsilon_2\omega_1^2)$, respectively. Important, for this case the results of the MPA differ from the results of EPA: index $p^{(1,2)}$ follows the curve $(\varepsilon_2 - \varepsilon_1)/(\varepsilon_1 + \varepsilon_2)$. Indeed, the predictability improvement is proportional to the amplitude of the coupling function and does not depend on its period (see caption to Fig. 2). Thus, MPA fails to reveal the asymmetry in coupling functions $f_{1,2}$. We note that the difference in estimates obtained by EMA and MPA may be used to extract information about the coupling function.

The above considerations were tested with the model (9),

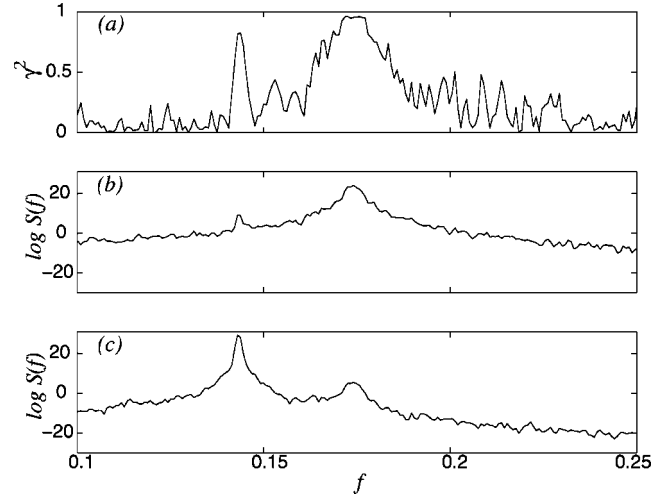


FIG. 7. Coherence function (a) and power spectra (b),(c) for two coupled oscillators. High coherence is seen around the natural frequencies of oscillators $\omega_{1,2}/2\pi$.

for which parameter values are $\omega_1 \approx 0.4$, $\omega_2 \approx 1.2$, $b=0$, $\varepsilon_1=0.01$, and ε_1 varied in the range from 0 to 0.018.

C. A note on more complex cases

In our tests of the techniques we always assumed that we deal with two coupled oscillators. In real-world applications we nevertheless can encounter more complex situations, e.g., when two systems are a part of a complex oscillatory network. Here, we comment on several important cases.

Uncoupled systems. Our algorithms cannot properly treat this situation. Hence, one should check whether both $c_{1,2}$ are close to zero and, if the presence of interaction is not obvious *a priori*, it is recommended to conduct first standard cross correlation (or other) analysis to check whether the two signals are inter-related.

Two coupled oscillators versus two uncoupled oscillators under common forcing. Two noninteracting systems can be driven by a common force. Certainly, in this case estimation of directionality indices is senseless. In order to exclude this case, we can exploit the cross-spectrum analysis, as illustrated by the following example. We simulate the output $x_{1,2}$ of two coupled noisy van der Pol oscillators

$$\ddot{x}_{1,2} - 0.2(1 - x_{1,2}^2)\dot{x}_{1,2} + \omega_{1,2}^2 x_{1,2} + \varepsilon_{1,2}(\dot{x}_{2,1} - \dot{x}_{1,2}) + \xi_{1,2} = 0,$$

to be compared with the output of two uncoupled systems under common driving

$$\ddot{x}_{1,2} - 0.2(1 - x_{1,2}^2)\dot{x}_{1,2} + \omega_{1,2}^2 x_{1,2} + \varepsilon_{1,2}\dot{x}_3 + \xi_{1,2} = 0,$$

where

$$\ddot{x}_3 - 0.2(1 - x_3^2)\dot{x}_3 + \omega_3^2 x_3 + \xi_3 = 0$$

and $\omega_1=0.9$, $\omega_2=1.1$, $\omega_3=1$, $\varepsilon_{1,2}=0.05$, and intensities of noise $\sigma_{1,2}=0.1$, $\sigma_3=0.5$. From the result of the cross-spectrum analysis shown in Figs. 7 and 8 we definitely can

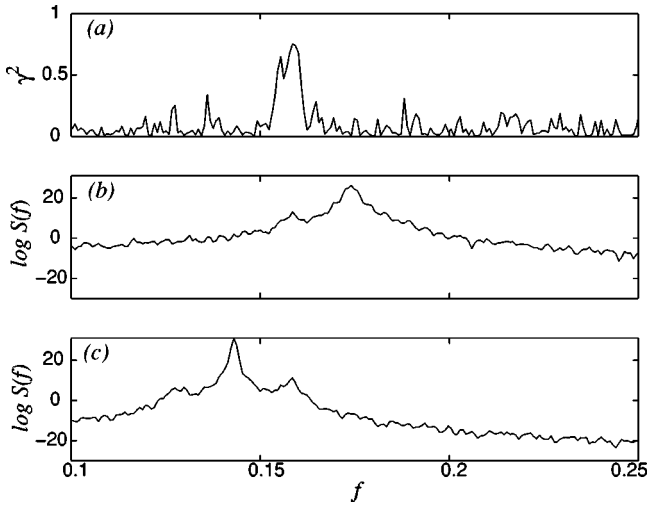


FIG. 8. Coherence function (a) and power spectra (b),(c) for two uncoupled oscillators driven by a common force. High coherence is observed at the frequency of that drive, but there is no coherence at the frequencies of oscillators. (Note that the frequency peak corresponding to the drive is barely seen in power spectra because the drive is very noisy.)

distinguish these two cases.

Three oscillators in a ring. Finally, we perform a frequently used test and consider three noisy van der Pol oscillators with unidirectional coupling, arranged in a ring (Fig. 9):

$$\ddot{x}_i - 0.2(1 - x_i^2)\dot{x}_i + \omega_i^2 x_i = \varepsilon \dot{x}_{(i+2) \bmod 3} + \xi_i.$$

Computing a directionality index for, say, oscillators 1 and 2, we expect this index to be between 0 and 1. Indeed, oscillator 2 acts on the oscillator 1 indirectly, via the system 3, and this action should be weaker than direct forcing of 2 by 1. To check this, we take the parameters $\omega_1 = 0.95$, $\omega_2 = 1.05$, $\omega_3 = 1$, $\varepsilon = 0.05$, a noise intensity 0.1, and estimate the d index from ≈ 500 oscillation periods; $\varepsilon = 0.05$, τ is of the order of the period. The results (see also Fig. 9) $d^{(1,2)} = 0.41$, $d^{(1,3)} = -0.7$, and $d^{(2,3)} = 0.57$ correctly reveal the direction of interaction in the ring structure. Next, we take identical systems, $\omega_1 = \omega_2 = \omega_3 = 1$, so that in the absence of noise the systems synchronize. With a sufficiently strong noise (with

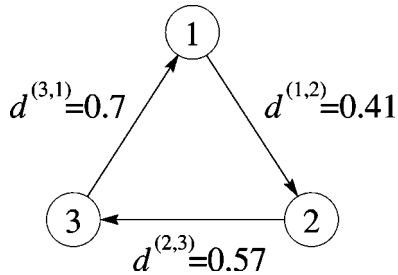


FIG. 9. Three oscillators arranged in a ring. The unidirectional (clockwise) coupling is revealed by pairwise estimation of the directionality index.

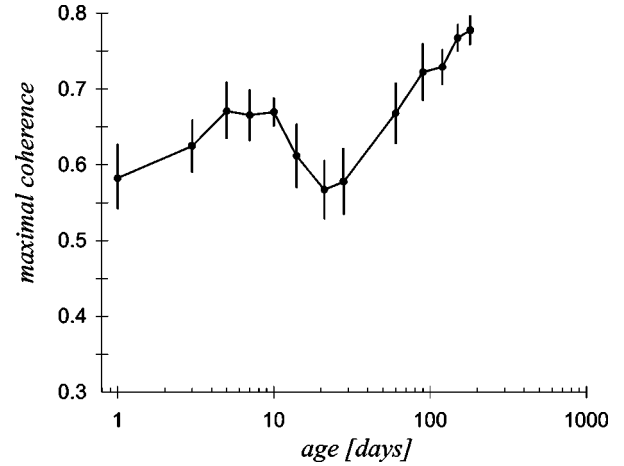


FIG. 10. Cross-spectral analysis demonstrates the presence of interaction between heart rate and respiration. For each of 16 subjects the maximal value of the coherence function was determined; the line and vertical bars show the mean and the standard error, respectively.

intensity 0.2), direction of coupling can be nevertheless detected: $d^{(1,2)} = 0.12$, $d^{(1,3)} = -0.19$, and $d^{(1,3)} = 0.27$.

IV. DIRECTIONALITY OF CARDIORESPIRATORY INTERACTION IN HEALTHY NEWBORNS

The goal of our experimental study is to clear the controversy concerning the direction of cardiorespiratory interaction. For this purpose we analyze bivariate data, namely, heart rate and respiration obtained from healthy newborns. The presence of interaction is indicated by the presence of respiratory sinus arrhythmia as well as the results of cross-spectral (Fig. 10) and synchronization [17] analysis performed on the same group of subjects. On the other hand, synchronous epochs are rather rare, so that the coupling can be considered weak. Next, we study the dependence of directionality indices on age as well as on heart rate and respiratory frequency.

A. Measurements and data analysis

We measured the electrocardiograms (ECG) using a bipolar limb lead (Biomonitor 501, Meßgerätewerk Zwönitz, Germany) and obtained thoracic respiration with the inductive plethysmographic method (Respirace, Studley Data Systems, Oxford, UK) in 25 newborn infants; data sets from five newborns are used in the present paper. Measurements were performed on each of the first 5 days of life, then every week and later monthly up to the 6th month of life. Data acquisition began 30–60 min after feeding, in the evening hours between 8 p.m. to 11 p.m., and took approximately 1 h. Data were stored on a digital audio tape (DAT) multichannel recorder (DAT, DTR-1800, biologic, France) for further analysis. The data were off-line digitized with a computer based monitoring system (XmAD, <ftp://sunsite.unc.edu/pub/Linux/science/lab/>) with a sampling rate of 1000 Hz.

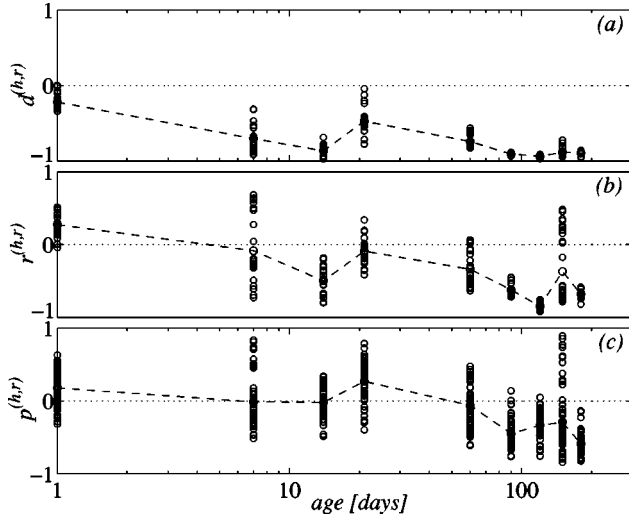


FIG. 11. Three directionality indices as a function of age for one subject. Each symbol shows the estimate of the respective index computed in a running window, the dashed lines connect the mean value for a particular day. Note the smaller variability of the d index.

An artifact free, ≈ 10 -min-long segment of each measurement was chosen for the further analysis; these segments correspond to the stage of quiet sleep. R waves were detected with the precision of 1 ms by means of a convolution technique applied to a fifth-order high-pass filtered ECG (20 ms moving average) and a typical QRS template. The instantaneous phase of the cardiac signal has been estimated according to

$$\phi_h(t) = 2\pi k + 2\pi \frac{t - t_k}{t_{k+1} - t_k}, \quad (12)$$

where t_k are the times of appearance of a k th R peak in the ECG. Phase of the respiratory signal has been obtained by means of Hilbert transform applied on the whole segment. Prior to phase derivation, the respiratory signal has been detrended (linear or polynomial, up to fourth order, trend was removed with manual check of all records), and smoothed using a second-order Savitzky-Golay filter of 501 data points length. See Refs. [5,11] for discussion of phase estimation techniques.

In order to trace the variation in the direction of coupling due to nonstationarity in the system, the corresponding indices were computed in a sliding window (with 3/4 overlap) and the average for each day was obtained. We found that all three methods provide consistent results (Fig. 11), supporting our assumption of weak coupling. Next, the stability of EMA and MPA with respect to parameter variation was checked. Comparing EMA and MPA we found that the d index is more stable with respect to parameter(s) variation than the p index; we remind that IPA has no parameters. In order to illustrate the robustness of EMA towards parameter variation, we focus on two distinct data sets from the same subject, corresponding to the first and the last (180th) recording day. An

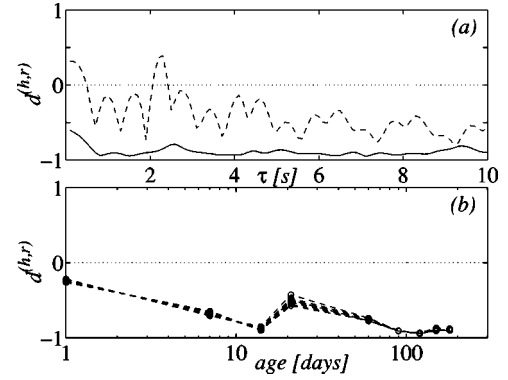


FIG. 12. Robustness of the estimates of the directionality index $d^{(hr)}$ with respect to parameters. (a) $d^{(hr)}$ vs τ for the first (dash-dotted line) and 180th (solid line) day of life; each estimate was computed from a data segment containing 200 heartbeats. (b) Influence of the window length. Open circles show the average of estimates of $d^{(hr)}$ computed with different window size (100, 200, \dots , 800 heartbeats).

≈ 100 -s-long segment was extracted from each of these two records, then $d^{(hr)}$ was computed for $\tau \leq 10$ s [see Fig. 12(a)]; the average interbeat interval was, respectively, $\langle T_h \rangle = 0.46$ s and $\langle T_h \rangle = 0.54$ s. A good stability of directionality index estimates with respect to the window size is reflected in Fig. 12(b). Further, data sets for five babies have been analyzed, with the window length corresponding to 200 heartbeats and τ taken as the average cardiac cycle within a window.

B. Results and discussion

Below we present only the results of the EMA approach (d index). This choice is motivated by our interest in the

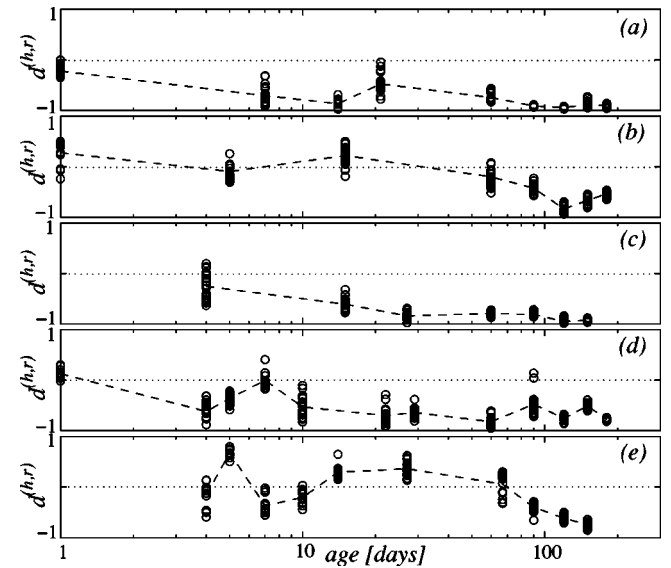


FIG. 13. Directionality index $d^{(hr)}$ versus age (log scale) for five newborns. Symbols show the values obtained from different windows; dashed lines show the average (for a certain day) values. All subjects demonstrate tendency towards unidirectional coupling (respiration drives heartbeat) with maturation.

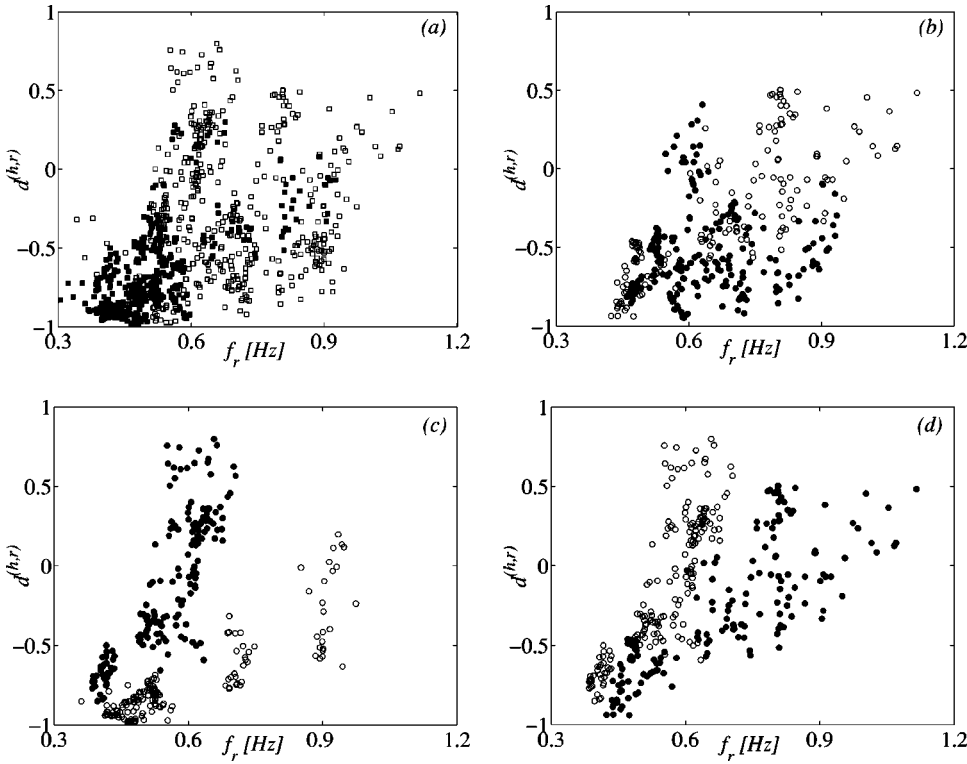


FIG. 14. Scatter plots of the $d^{(h,r)}$ index versus breathing frequency (f_r) have a characteristic ν shape. (a) All five subjects together. Opened and filled squares denote the estimates during the first month and 2–6 months, respectively. (b), (c), and (d) show the results for two subjects (denoted by different symbols). One can see that the points from some subjects fall only onto one branch of the ν curve (c), while the estimates from other subjects fall onto both branches (b). In one subject the first days fall onto one, others fall onto the second stripe (d).

dependence of the directionality on both respiratory frequency and heart rate. We remind also that d index does not directly include oscillator frequencies [cf. Eqs. (10),(11)] what results in a smaller variability of its estimates (cf. Fig. 11).

The main results are summarized in Fig. 13 clearly indicating the evolution from an approximately symmetric interaction during the first days of life to a dominant unidirectional coupling (respiration drives the heart rate) at the age of 6 months. Next, we analyzed the dependence of the directionality index $d^{(h,r)}$ on the frequency of respiration f_r and on heart rate f_h . No dependence between $d^{(h,r)}$ and f_h was seen, whereas the plot of $d^{(h,r)}$ vs f_r displays a characteristic ν shape [Fig. 14(a)]. It can be seen that, for all measurements with $f_r < 0.5$ Hz the interaction occurs dominantly in one direction, from respiration to heart rate. We suggest the following explanation. The cardiac influence on respiration is weak and frequency independent, while the coupling from the respiration to heart rate is similar to a low-pass filter. Then, for low frequencies ($f_r \approx 0.5$ Hz in our case) the respiratory driving effect is relatively strong compared with the strength of the cardiac influence; correspondingly, the directionality index is close to -1 . For higher frequencies, the signal from the respiratory center [35] is attenuated and therefore the interaction appears as nearly symmetrical. This explanation is supported by the fact that variability of d index estimates is larger for higher frequencies (influence of noise on the estimate of an index is stronger for weak coupling, see discussion in the Sec. III).

The basis of the low-pass behavior of the information transmission channel can be found in the physiological mechanisms of the coupling. Indeed, signals from the vagal nerve to the sinus node are transmitted by means of the neu-

rotransmitter acetylcholine. The release and the enzymatic degradation of the acetylcholine is frequency limited [37]. Note also, that respiratory sinus arrhythmia is a frequency-dependent phenomenon as well [14].

The presence of two branches in the ν -shaped plot of d index vs f_r indicates two possible modes of interaction, characterized by different characteristics of the low-pass filter (see Fig. 14). At very young ages (first week of life), the value of the cutoff frequency appears to be lower. Maturation of the functions of the central nervous system as well as cardiovascular adaptation processes to extrauterine conditions such as closure of fetal shunts may account for this finding. Correlation to hemodynamic data could give further insight into this hypothesis. Another possible explanation of the existence of two modes of interaction may be related to different substages of quiet sleep [38].

In summary, our results support the “irradiation theory” in the sense that there is a clear effect of respiration on heart rate. However, at physiological conditions, characterized by high breathing rates, this unidirectional action is abolished. The reason for this abolishment is explained by the well-known neurotransmitter kinetics of acetylcholine at the vagal-atrial junction. To reveal mechanisms responsible for the ν shape of the dependence of the directional index on breathing frequency further investigations are necessary.

V. CONCLUSIONS

We have proposed and analyzed approaches for identification of direction of weak coupling between two self-sustained oscillators. We have compared the efficiency of three algorithms and have shown that they can be used for analysis of real-world data. One algorithm EMA requires

only one parameter, is generally more stable towards its variation and easier to use than the algorithm based on the idea of mutual predictability. The essential advantage of the proposed method IPA is that it has no parameters. More important, all methods work with rather short and noisy records, that makes them suitable for applications to biological, geophysical, astrophysical, and other real-world signals.

Application of the considered methods to a particular problem, analysis of cardiorespiratory coupling, revealed that this interaction is age dependent: it evolves from approximately symmetric coupling during the first days of life to unidirectional after 6 months of age. Moreover, the depen-

dence of the directionality index on the respiratory frequency indicates the possible existence of two regimes of interaction.

ACKNOWLEDGMENTS

We are indebted to A. Pikovsky for constant help and valuable comments and to P. Ivanov and F. Starmar for a careful reading of the manuscript and useful remarks. We gratefully acknowledge discussions with R. Friedrich, J. Kurths, U. Parlitz, G. Osipov, T. Schreiber, P. Tass, and M. Zaks. M.R. was supported by EU Network COSYS of SENS.

-
- [1] H.D.I. Abarbanel, *Analysis of Observed Chaotic Data* (Springer-Verlag, New York, 1996); H. Kantz and T. Schreiber, *Nonlinear Time Series Analysis* (Cambridge University Press, Cambridge, U.K., 1997).
- [2] N.F. Rulkov, M.M. Sushchik, L.S. Tsimring, and H.D.I. Abarbanel, *Phys. Rev. E* **51**, 980 (1995); L. Kocarev and U. Parlitz, *Phys. Rev. Lett.* **76**, 1816 (1996).
- [3] M.G. Rosenblum, A.S. Pikovsky, and J. Kurths, *Phys. Rev. Lett.* **76**, 1804 (1996).
- [4] A.S. Pikovsky, M.G. Rosenblum, G.V. Osipov, and J. Kurths, *Physica D* **104**, 219 (1997); A. Pikovsky, M. Rosenblum, and J. Kurths, *Int. J. Bifurcation Chaos Appl. Sci. Eng.* **10**, 2291 (2000).
- [5] A. Pikovsky, M. Rosenblum, and J. Kurths, *Synchronization, A Universal Concept in Nonlinear Sciences* (Cambridge University Press, Cambridge, 2001).
- [6] S.J. Schiff, P. So, T. Chang, R.E. Burke, and T. Sauer, *Phys. Rev. E* **54**, 6708 (1996); M. Le van Quyen, C. Adam, M. Baulac, J. Martinerie, and F. Varela, *Brain Res.* **792**, 24 (1998); J. Arnhold, P. Grassberger, K. Lehnertz, and C. Elger, *Physica D* **134**, 419 (1999); R. Quian Quiroga, J. Arnhold, and P. Grassberger, *Phys. Rev. E* **61**, 5142 (2000); A. Schmitz, *ibid.* **62**, 7508 (2000); F. Drepper, *ibid.* **62**, 6376 (2000).
- [7] M. Rosenblum, A. Pikovsky, and J. Kurths, *IEEE Trans. Circuits Syst., I: Fundam. Theory Appl.* **44**, 874 (1997).
- [8] C. Schäfer, M.G. Rosenblum, J. Kurths, and H.-H. Abel, *Nature (London)* **392**, 239 (1998).
- [9] P. Tass, M. Rosenblum, J. Weule, J. Kurths, A. Pikovsky, J. Volkman, A. Schnitzler, and H.-J. Freund, *Phys. Rev. Lett.* **81**, 3291 (1998).
- [10] C. Schäfer, M. Rosenblum, H.-H. Abel, and J. Kurths, *Phys. Rev. E* **60**, 857 (1999).
- [11] M.G. Rosenblum, A.S. Pikovsky, J. Kurths, C. Schäfer, and P. A. Tass, in *Neuro-informatics*, edited by F. Moss and S. Gielen, *Handbook of Biological Physics*, Vol. 4 (Elsevier, New York, 2001), pp. 279–321.
- [12] Y. Kuramoto, *Chemical Oscillations, Waves, and Turbulence* (Springer, Berlin, 1984).
- [13] M.G. Rosenblum and A.S. Pikovsky, *Phys. Rev. E* **64**, 045202 (2001).
- [14] A. Angelone and N. Coulter, *J. Appl. Physiol.* **19**, 479 (1964).
- [15] H. Pessenhofer and T. Kenner, *Pfluegers Arch.* **355**, 77 (1975); T. Kenner, H. Pessenhofer, and G. Schwaberg, *ibid.* **363**, 263 (1976); K.H. Stutte and G. Hildebrandt, *ibid.* **289**, R47 (1966); F. Raschke, in *Temporal Disorder in Human Oscillatory Systems*, edited by L. Rensing, U. an der Heiden, and M. Mackey, *Springer Series in Synergetics Vol. 36* (Springer-Verlag, Berlin, 1987), pp. 152–158; F. Raschke, in *Rhythms in Physiological Systems*, edited by H. Haken and H.P. Koepchen, *Springer Series in Synergetics Vol. 55* (Springer-Verlag, Berlin, 1991), pp. 155–164; D. Hoyer, O. Hader, and U. Zwiener, *IEEE Eng. Med. Biol. Mag.* **16**, 97 (1997); M. Schiek, F.R. Drepper, R. Engbert, H.-H. Abel, and K. Suder, in *Nonlinear Analysis of Physiological Data*, edited by H. Kantz, J. Kurths, and G. Mayer-Kress (Springer, Berlin, 1998), pp. 191–209; H. Seidel and H.-P. Herzel, *IEEE Eng. Med. Biol. Mag.* **17**, 54 (1998).
- [16] M. Bračič and A. Stefanovska, *Physica A* **283**, 451 (2000).
- [17] R. Mrowka, A. Patzak, and M.G. Rosenblum, *Int. J. Bifurcation Chaos Appl. Sci. Eng.* **10**, 2479 (2000).
- [18] H.P. Koepchen, *Die Blutdruckrhythmik* (Dr. Dietrich Steinkopff Verlag, Darmstadt, 1962).
- [19] R.K. Otnes and L. Enochson, *Digital Time Series Analysis* (Wiley, New York, 1972).
- [20] B. Pompe, *J. Stat. Phys.* **73**, 587 (1993).
- [21] H. Voss and J. Kurths, *Phys. Lett. A* **234**, 336 (1997).
- [22] T. Schreiber, *Phys. Rev. Lett.* **85**, 461 (2000); M. Paluš, V. Komárek, Z. Hrnčíř, and K. Štěrbová, *Phys. Rev. E* **63**, 046211 (2001).
- [23] A.S. Pikovsky, *Sov. J. Commun. Technol. Electron.* **31**, 81 (1986).
- [24] R. Friedrich, S. Siegert, J. Peinke, S. Lück, M. Siefert, M. Lindemann, J. Raethjen, G. Deuschl, and G. Pfister, *Phys. Lett. A* **271**, 217 (2000).
- [25] Practically, for discrete data, this can be done in the following way. For any t_k we find t_j such that $\phi(t_j) \leq \phi(t_k) + 2\pi$ and $\phi(t_{j+1}) > \phi(t_k) + 2\pi$. Then t' correspondent to $\phi = \phi(t_k) + 2\pi$ is obtained via interpolation between t_j and t_{j+1} . If the sampling rate is high, simple linear interpolation suffices, otherwise spline interpolation (using several points around t_j) is recommended; this procedure also reduces the effect of noise.
- [26] C. Granger, *Econometrica* **37**, 424 (1969).
- [27] M. Wiesenfeldt, U. Parlitz, and W. Lauterborn, *Int. J. Bifurcation Chaos Appl. Sci. Eng.* **11**, 2217 (2001).
- [28] U. Feldmann and J. Bhattacharya (unpublished); B. Schack and M. Arnold (private communication).
- [29] We emphasize that the phases are considered unwrapped when

we compute the phase increase Δ , and wrapped when we search for close neighbors. Considering the averaging, we note that for short records the number of mutual neighbors is small, and the statistics is therefore poor, and the predictability improvement is reduced. To compensate this, we used only m out of l points in averaging involved in computation of the univariate prediction error.

- [30] Indeed, for the simplest case of sine coupling function, $f_{1,2} = \sin(\phi_{2,1} - \phi_{1,2})$, in the synchronous regime the constant phase difference is $\phi_2 - \phi_1 = \arcsin(\omega_2 - \omega_1)/(\varepsilon_2 + \varepsilon_1)$, and we cannot extract information on $\varepsilon_{1,2}$ separately.
- [31] K.K. Likharev, *Dynamics of Josephson Junctions and Circuits* (Gordon and Breach, Philadelphia, 1991).
- [32] V.S. Afraimovich, V.I. Nekorkin, G.V. Osipov, and V.D. Shalfeev, *Stability, Structures, and Chaos in Nonlinear Synchronization Networks* (World Scientific, Singapore, 1994).
- [33] We use the index $\rho^2 = \langle \cos[\phi_1(t) - \phi_2(t)] \rangle^2 + \langle \sin[\phi_1(t) - \phi_2(t)] \rangle^2$, where $\langle \rangle$ denote time average, see Refs. [11,34].
- [34] E. Rodriguez, N. George, J.-P. Lachaux, J. Martinerie, B. Renault, and F.J. Varela, *Nature (London)* **397**, 430 (1999).
- [35] Current models of respiration imply that the respiratory rhythm is generated in the brain stem, in a network, which includes also neurons modulating heart rate [36].
- [36] D.W. Richter and K.M. Spyer, in *Central Regulation of Autonomic Functions*, edited by A.D. Loewy and K.M. Spyer (Oxford University Press, New York, 1990), pp. 189–207.
- [37] W. Osterrieder, Q.F. Yang, and W. Trautwein, *Pfluegers Arch.* **389**, 283 (1981); M.R. Boyett and A. Roberts, *J. Physiol. (London)* **393**, 171 (1987); M.H. Chen, R.D. Berger, J.P. Saul, K. Stevenson, and R.J. Cohen, *Comput. Cardiol.* **13**, 149 (1987); F. Dexter, Y. Rudy, and G.M. Sidel, *Am. J. Physiol.* **266**, H298 (1994).
- [38] Quiet sleep in young infants is usually not further classified into substages in clinical practice.